Original Article

JCBFM

Journal of Cerebral Blood Flow & Metabolism
2021, Vol. 41(2) 236–252

DOI: 10.1177/0271678X20914179
journals.sagepub.com/home/jcbfm
SAGE

Dynamic capillary stalls in reperfused ischemic penumbra contribute to injury: A hyperacute role for neutrophils in persistent traffic jams

Şefik E Erdener[1,2], Jianbo Tang[1,2], Kıvılcım Kılıç[1], Dmitry Postnov[1,3], John T Giblin[1], Sreekanth Kura[1], I-chun A Chen[1], Tuğberk Vayisoğlu[1], Sava Sakadžić[2], Chris B Schaffer[4] and David A Boas[1]

Abstract

Ever since the introduction of thrombolysis and the subsequent expansion of endovascular treatments for acute ischemic stroke, it remains to be identified why the actual outcomes are less favorable despite recanalization. Here, by high spatio-temporal resolution imaging of capillary circulation in mice, we introduce the pathological phenomenon of dynamic flow stalls in cerebral capillaries, occurring persistently in salvageable penumbra after reperfusion. These stalls, which are different from permanent cellular plugs of no-reflow, were temporarily and repetitively occurring in the capillary network, impairing the overall circulation like small focal traffic jams. In vivo microscopy in the ischemic penumbra revealed leukocytes traveling slowly through capillary lumen or getting stuck, while red blood cell flow was being disturbed in the neighboring segments under reperfused conditions. Stall dynamics could be modulated, by injection of an anti-Ly6G antibody specifically targeting neutrophils. Decreased number and duration of stalls were associated with improvement in penumbral blood flow within 2–24 h after reperfusion along with increased capillary oxygenation, decreased cellular damage and improved functional outcome. Thereby, dynamic microcirculatory stall phenomenon can be a contributing factor to ongoing penumbral injury and is a potential hyperacute mechanism adding on previous observations of detrimental effects of activated neutrophils in ischemic stroke.

Keywords

Cerebral ischemia, capillary, microcirculation, neutrophil, stall

Received 22 October 2019; Revised 18 February 2020; Accepted 18 February 2020

Introduction

Over the last years, there has been an expansion of endovascular recanalization practices for acute ischemic stroke with pivotal clinical trials showing functional benefit.[1] Selection of patients with salvageable penumbra using multimodal imaging technologies not only improved the success rate but has also extended the therapeutic window up to 24 h in eligible.[1,2] Still, however, even when enrollment and recanalization timing and efficiency are optimal, nearly half of the patients do not experience clinical improvement.[3] This lower-than-expected efficacy has been attributed to subsequent arterial reocclusion or to the "no-reflow"

[1]Neurophotonics Center, Department of Biomedical Engineering, Boston University, Boston, MA, USA
[2]Optics Division, Athinoula A. Martinos Center for Biomedical Imaging, Massachusetts General Hospital, Harvard Medical School, Charlestown, MA, USA
[3]Institute of Biomedical Sciences, Faculty of Health and Medical Sciences, Copenhagen University, Copenhagen, Denmark
[4]Meinig School of Biomedical Engineering, Cornell University, Ithaca, NY, USA

Corresponding author:
Şefik E Erdener, Department of Biomedical Engineering Boston University 44 Cummington Mall, Boston, MA 02215, USA.
Email: evrenerdener@gmail.com

phenomenon, when microcirculatory flow is not restored in small arterioles and capillaries, despite full recanalization of the large artery.[3–5] Indeed, adequacy of capillary perfusion seems to be a better predictor of clinical outcome after endovascular recanalization.[3–5] Previously, sustained pericyte contraction after ischemia–reperfusion has been shown to cause red blood cell (RBC) entrapment in the ischemic tissue.[6] Polymorphonuclear leukocytes have been recognized as another factor blocking the capillary lumen as they are activated and extravasated into the parenchyma,[7–9] contributing to the tissue injury. However, while these static observations are very informative, we know that capillary flow patterns are as important as their structure for maintaining tissue oxygen delivery.[10] This recognition motivated us to investigate the temporal dynamics of the ischemia-related persistent capillary perfusion loss, i.e. whether the capillary occlusions are permanent or transient and repetitive in a particular capillary segment. Specifically, we aimed to extend our recent systematic analyses of spontaneous temporary RBC flow interruptions in cerebral capillaries, i.e. stalls, in healthy animals[11] to the ischemic tissue early after reperfusion and tested if neutrophils, a large and less deformable cell moving rather slowly in microvasculature,[12] could be an aggravating factor for the capillary stall events. By analogy, dynamic stalls occurring above a critical level in the ischemic penumbra would indicate micro-level traffic jam-like formations due to extremely heterogeneous flow, as road traffic models demonstrate even tiny irregularities in vehicle flow can cause expanding flow redistributions, rapidly growing instability and subsequent accumulation of flow blocks.[13] We also wanted to evaluate the potential contribution of those microcirculatory abnormalities to the ongoing damage in the dysfunctional and critically hypoperfused but salvageable tissue, the ischemic penumbra,[5] rather than being a bystander phenomenon of the already infarcted ischemic core. To address these questions, we took advantage of in vivo microscopic imaging, such as optical coherence tomography (OCT) and two-photon microscopy (TPM), using a mouse model of transient distal middle cerebral artery occlusion (dMCAO).

Materials and methods

Animals and surgery

All experiments were approved by the Institutional Animal Care and Use Committees of Massachusetts General Hospital and Boston University. Experiments were conducted following the Guide for the Care and Use of Laboratory Animals and reported in compliance with the ARRIVE guidelines.

For this study, 12–16-week-old C57BL/6 mice (total of 48 animals, male, Charles River Laboratories) were used. Animals were housed under diurnal lighting conditions with free access to food and water. Surgery and experiments were performed under isoflurane anesthesia (2–3% induction, 1–2% maintenance, in 60% nitrogen, 40% oxygen mixture). An aluminum bar was glued to the skull for head fixation. A 2-mm craniotomy was opened in the temporal bone over the dMCA, with dura intact. Next, another 4-mm craniotomy was opened in right frontoparietal area over the edge of the MCA-supplied cortex. The brain was covered with 0.7% agarose solution, then with a 5-mm glass coverslip, sealed with dental cement. The animal was then placed under the imaging system. We waited for at least an hour for stabilization of the cerebral blood flow (CBF) until we started the baseline imaging.

Transient distal MCAO model

For initiation of ischemia, an occlusion device (Figure 1(c)) made by the fusion of two blunted borosilicate glass micropipettes was positioned over the dMCA with a micromanipulator (YOU-1, Narishige, Japan).[14] After baseline imaging, the pipette was gently advanced to press on the MCA trunk, at the point where it crossed the inferior cerebral vein, until blood flow dropped. CBF was monitored via laser speckle contrast imaging in real-time to confirm ischemia initiation and maintenance (Figure 1(h)). Ischemia was confirmed by checking the real-time relative CBF maps indicating at least 50% CBF decrease in MCA-supplied cortex along with disappearance of flow in at least one pial MCA branch. Maintenance of ischemia was also ensured by stability of the oligemia in MCA-supplied cortex and exclusion of unintended recanalization of MCA which immediately resulted in a prominent reflow in MCA branches. After 1 h of ischemia, the pipette was drawn back to recanalize the artery. In 22 animals, experiments were terminated ~2.5 h after reperfusion because of invasive blood pressure monitoring; these animals were used for stall parameter and CBF measurements, pO_2 measurements and Rhodamine-6G imaging until the 2nd after reperfusion. A total of 18 animals survived overnight for one-day capillary flow measurements, functional assessment, propidium iodide staining or infarct volume determination. Animals intraperitoneally injected with propidium iodide ($n = 3$ per group) (300 µl of 1 mg/ml PI solution (Molecular Probes) diluted with 300 µL injectable sterile saline) were transcardially perfused 4 h later with a fluorescent gel containing fluorescein isothiocyanate (FITC)-albumin conjugate. In sham animals ($n = 6$), all surgical procedures were performed, but the blunted pipette

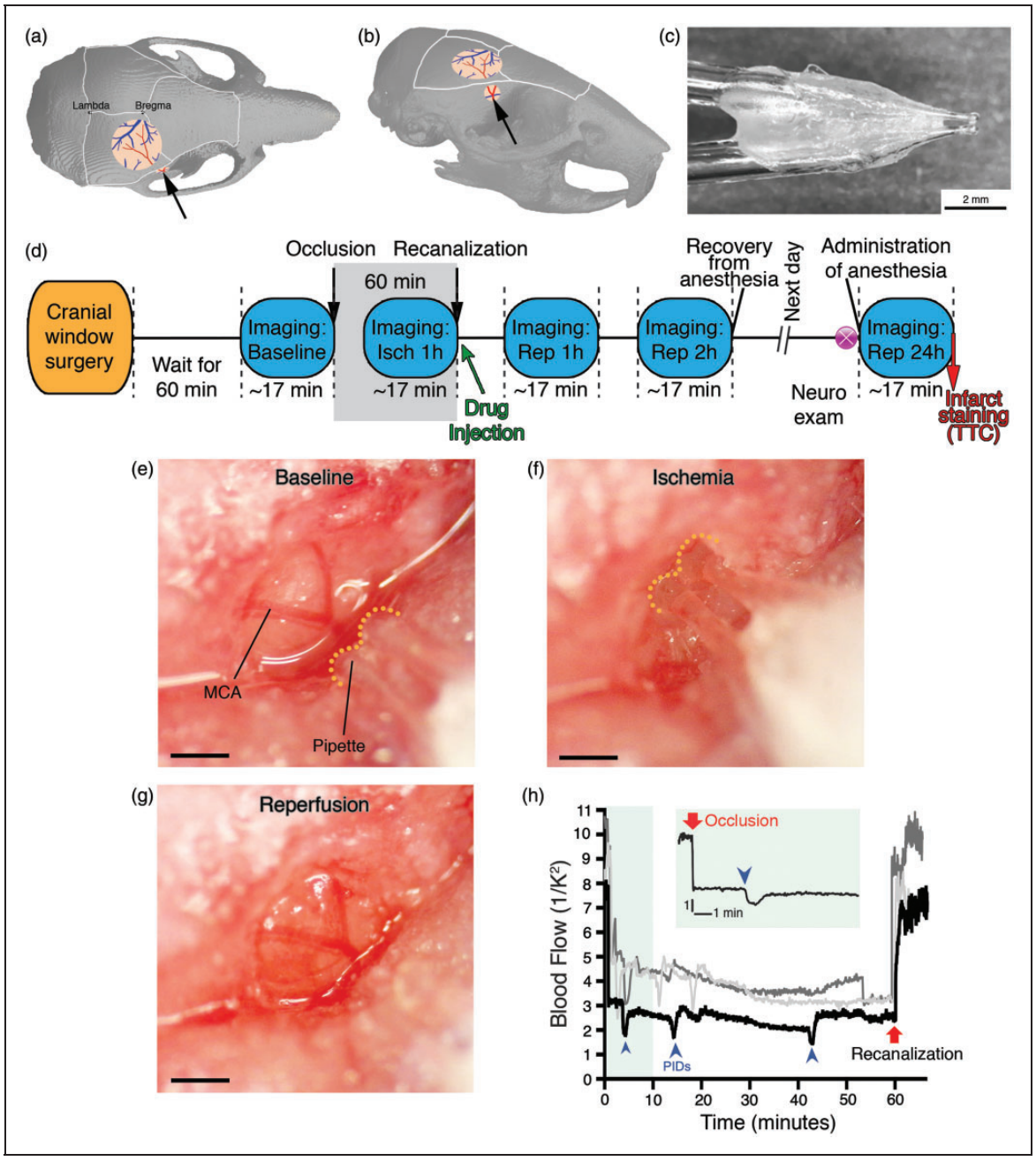

Figure 1. (a,b) Diagrams showing the top and oblique views of the mouse skull, with the locations of two cranial windows indicated. Black arrow shows the direction of compression over the distal MCA at the bifurcation point. (c) Close-up view of the occlusion device, made by fusion of two blunted micropipettes with an approximate 10-degree angle at the tip. (d) Experimental timeline showing the surgery, MCA occlusion and recanalization, drug injection imaging time points and study end points. (e–g) Color photographs acquired under the surgical microscope, showing the experimental procedure of dMCAO and recanalization (Scalebars: 500 μm). The tip of the micropipette device is outlined with yellow dotted line. After recanalization, there was no visible injury to the MCA, apart from minimal bruising in the dura. (h) Representative blood flow tracings from three separate experiments measured with laser speckle contrast imaging during MCAO and initial reperfusion. Individual experiments are plotted with different colors. Please note that the Y-axis shows the blood flow index ($1/K^2$) values which should be evaluated relative to baseline, which can differ across animals. Each blood flow index value is the average of pixels in a 0.2×0.2 mm^2 region of interest placed in the MCA supplied zone. Shortly after the initial dip of blood flow with dMCAO, we detected recurrent peri-infarct depolarizations (PIDs, blue arrowheads) characterized by their oligemic transients lasting 1–2 min. Inset is the extension of the green-shaded area in the plot.

compression was applied over the dura adjacent to the MCA, with no compression of vascular structures. Two MCAO animals with complete data sets were excluded during data quality assessment, because of insufficient level of oligemia (above 70% of baseline during arterial compression). Data from all other animals were processed and included in analysis.

Antibody treatment

For targeting of leukocytes, anti-Ly6G antibody (2 mg/kg, BD Biosciences) was administered retroorbitally over 30 s, ~3 min after reperfusion ($n = 17$ mice). For the control group, isotype control antibody, (2 mg/kg, BD Biosciences) ($n = 19$ mice) was injected; 100 µL antibody was diluted with 50 µL sterile injectable saline. Animals were randomized into treatment groups before experiments. Injection was performed by the investigator performing the dMCAO, who was blinded to the injection type.

Optical coherence tomography

A spectral-domain OCT system (1310 nm center wavelength, bandwidth 170 nm, Thorlabs Telesto III) was used for imaging of the cerebral cortex. OCT-angiograms were constructed by a decorrelation-based method.[15] In this study, imaging regions of interest (ROI) were raster scanned at different pixel resolutions. Maximum intensity projections (MIP) over a depth range of 150–250 μm beneath the brain surface were extracted from angiogram volumetric data for analysis as these layers provided a high-quality angiogram signal from capillaries. Phase-resolved Doppler OCT (prD-OCT)[16] was utilized to quantify the axial blood flow velocity in penetrating vessels. Please refer to the Supplementary Online Material for details on OCT acquisition and data processing.

For each timepoint during the experiments (baseline, ischemia, reperfusion-at 1 h, 2 h and 24 h), a new OCT dataset was acquired. Each OCT dataset consisted of one time series (60 consecutive volumes) of narrow-field data, five volumes of wide-field data (both for 5× and 10×) and one volume of PrD-OCT data. The same cortical region was repeatedly imaged for experimental timepoints and readjustments were not necessary since the animal was not removed from the imaging system during experiments (apart from repeat imaging at 24 h after reperfusion). On a few occasions, minor shifts in ROI location were necessary after baseline acquisition, to acquire the targeted zone of the core-penumbra boundary after the onset of ischemia.

Two-photon microscopy

A commercial laser scanning TPM system (Bruker Investigator) with an integrated Becker and Hickl TCSPC FLIM module was used with a Nikon, 16×, 0.8 NA, water-immersion objective. For in vivo visualization of leukocytes (5 mice), 100 µL of Rhodamine-6G (Sigma-Aldrich, R4127, 0.05% in PBS, freshly prepared) was injected retro-orbitally, 5 min before imaging. The dye was excited at 830 nm. For capillary pO_2 determination, oxygen-sensitive dye PtP-C343 (60 mg/ml, 120 µL) was retro-orbitally injected (6 mice). PtP-C343 fluorescence visualized the plasma, while blood cells remained unstained. Capillary fluorescence was initially imaged for anatomic guidance. pO_2 determination was done at all visible microvasculature segments, including precapillary arterioles, capillaries and postcapillary venules (microvasculature segments with diameters between 5 µm and 15 µm, regardless of branching order), across a single focal plane (at 120–170 µm deep) over a ~440 × 440 µm imaging field of view; 20–30 points inside capillaries were measured at each imaging region, the exact number depending on the number of visible capillaries. Segments with no reliable measurement of phosphorescence decay due to technical issues, resulting in insufficient photon counts, were excluded. Phosphorescence lifetime measurement in capillaries was performed as reported previously.[17] Please refer to the Supplementary Material for details on TPM data acquisition.

Quantification of stalls

Quantitative analyses of capillary stalls were performed as reported previously (in 24 MCAO mice, 4 sham mice).[11] In angiogram time-series, stalling capillary segments could be easily identified as a sudden drop in signal intensity; disappearance and reappearance of flowing RBCs in individual segments could be observed. The segments analyzed were defined as capillaries that do not extend beyond a branching point, with at least a 25 µm length in the transverse plane projection. Each stall was manually marked and analyzed using custom MATLAB codes. Please refer to Supplementary Material for details on analysis.

Statistical analyses

Data analysis was performed in a blinded fashion with respect to the treatment group. Sample sizes were estimated with power analysis using data from preliminary experiments, taking standard deviation of CBF and stall parameters into consideration. Independent groups (isotype control vs. anti-Ly6G) were compared by Mann–Whitney U test unless otherwise indicated. Dependent comparisons between different time points

were done by Friedman test followed by Dunn's multiple comparisons test for comparisons with baseline. Results were expressed as mean ± standard deviation, unless otherwise indicated.

Results

Mapping the salvageable ischemic penumbra with OCT

We utilized a mouse model of transient dMCAO by applying mechanical compression with a device made by fusing two glass micropipettes with blunted tips (Figure 1(a) to (c)), based on a previously reported model[14,18,19] that ensured stable occlusions for 60 min. Complete reperfusion was achieved simply by the release of compression after 1 h, without any requirement for a thrombolytic agent.[14,19] CBF was continuously monitored by laser speckle contrast imaging to ensure successful occlusion and reperfusion (Supplementary Movies 1 and 2, Figures 1(h) and 2 (a) to (c)). The occlusion was considered successful (in ~95% of trials) if at least one pial MCA segment within the cranial window had absence of blood flow, in addition to opening of collaterals from the anterior cerebral artery (ACA)-supplied zone (Supplementary Movie 1). Another criterion for successful occlusion was appearance of abnormal optical scattering measured by OCT (see below). Recanalization was successful in all experiments (demonstrated by blood flow recovery in pial MCA branches) with no visible damage to the dMCA (Figure 1(g)). Since all animals had different pial vascular anatomy and collateral supply, and we wanted to study the capillary flow in the penumbra tissue immediately next to the evolving core in every single experiment, we had to control for variations that could result in different spatial distributions of varying grades of oligemia. Real-time monitoring of CBF changes by laser speckle imaging revealed the baseline flow map and postischemic collateral flow, guiding the subsequent OCT imaging of microcirculation. Longitudinal OCT imaging within this penumbral zone at baseline and different time points during vascular occlusion/reperfusion (Figure 1(d)) quantified CBF, visualized capillary flow and optical attenuation changes. OCT imaging properly mapped the infarct area inside the MCA-supplied ischemic cortex (Figure 2(g) and (h), Supplementary Figures S2 and S3), helping us direct our further analyses to the core-penumbra transition zones on an individualized basis. Our dMCAO model also allowed the experiment without removing or repositioning the animal under the imaging equipment.

Approximately 60 min after the initiation of dMCAO, OCT angiograms demonstrated a severely compromised microvascular bed with almost no capillary perfusion in the ischemic core and relatively present, but still lower-than-baseline perfused capillary density in the penumbra region, surrounding the ischemic core (Figure 2(e)). We also detected an abnormal optical scattering within the ischemic core, allowing a clear distinction of the developing infarct within the hypoperfused MCA territory (Figure 2(g) and (h)). To quantify the scattering changes, the axial decay profile of the OCT signal amplitude was analyzed as a function of cortical depth by following the procedure outlined in a previous study.[20] The axial signal attenuation was prominently higher (i.e. had a higher axial decay slope) in the well-demarcated area with very low (or absent) capillary perfusion (the core) compared to the attenuation in the periinfarct penumbral zones (Figure 2(g) and (h), Supplementary Figure 2). These attenuation changes established 2 h after reperfusion overlapped with the infarcts demonstrated by TTC staining done shortly after in vivo imaging (Figure 2 (i)). Modeling the well-documented MRI-definition of diffusion-perfusion mismatch,[21] we identified our penumbral region of interest as the hypoperfused MCA region peripheral to the ischemic core border. The change in the slope of the axial OCT signal in the evolving infarct was not a direct result of CBF and/or blood volume changes as the attenuation changes did not synchronize with the loss of capillary flow (Supplementary Figure 3).

Phase-resolved Doppler OCT (prD-OCT) was used to quantify the velocity in individual penetrating arterioles under baseline and ischemic conditions, allowing us to calculate the CBF in a given region of interest (Figure 2(j) to (l)). Because of baseline variability in CBF, we expressed the subsequent ischemia and reperfusion values as normalized to baseline. This measure was used to compare blood flow changes in different experimental groups, as detailed below. Overall, within the ischemic core, blood flow was found to be decreased to 14 ± 4% of baseline during MCAO, while in penumbra it decreased to 39 ± 4% and these values were in agreement with previously reported levels in the similar models of cerebral ischemia.[22,23]

One hour after recanalization, we consistently detected a persisting lower-than-baseline capillary perfusion in the ischemic penumbra. These changes were not confounded by systemic physiological parameters, like oxygen saturation, heart rate, blood pressure and body temperature (Table 1). We then wanted to further evaluate the capillary-level flow dynamics in the ischemic penumbra, to understand if the low perfusion was simply due to permanent capillary occlusions or if the proposed dynamic stalls were contributing to an impairment in overall blood flow.

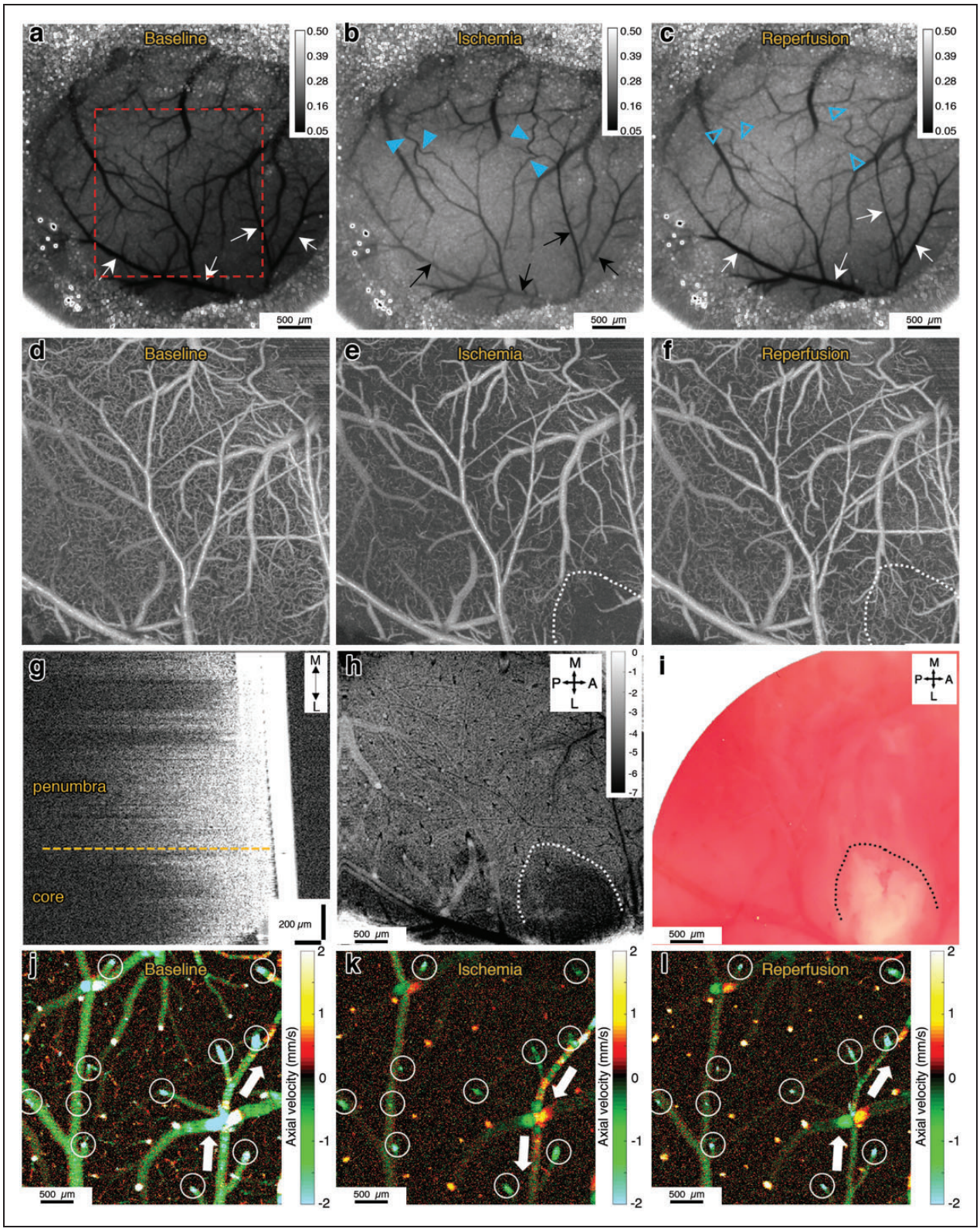

Figure 2. (a–c) Laser speckle contrast images showing the baseline, ischemia (end of 1st h) and reperfusion (after 1 h) conditions. Black and white arrows show the pial branches of the MCA. Darker colors indicate higher flow. After occlusion, we see decreased or absent flow in the pial MCA branches, and increased flow in collateral vessels (blue arrowheads) from the ACA-supplied region. After reperfusion, we see collateral flow prominently decreases (blue empty arrowheads). Scale bars: 500 μm. (d–f) OCT angiograms (average of 10 images) of the area shown in the red square in panel (a). Only RBC-perfused capillaries are visible in those images.

(continued)

Dynamic capillary stalls increase in ischemic penumbra and persist after reperfusion

In our preliminary experiments, OCT angiogram time series over ~6.5 min consistently showed very frequent transient RBC stalls (in comparison to baseline conditions from same animals and also to our experience under physiological conditions[11]) in individual capillaries during ischemia (Figure 3(a) to (g)) and for at least 2 h after reperfusion. Interestingly, this dynamic information was lost if capillary angiograms were averaged, as commonly done with OCT angiogram data to increase the signal-to-noise ratio (Supplementary Movie 3). This implied that even the visible capillaries in ischemic penumbra in averaged OCT angiograms were not flowing optimally but were showing high temporal flow heterogeneity per each segment. In some segments in penumbra, 2 h after canalization, RBC flow was stopping for more than 5 min, then restarting before another interruption settled in (Figure 3(h)). The minimum duration of a stall that we could indicate in our experiments, limited by the OCT frame rate, was 6.5 s. Any contributing effect of a coincident peri-infarct depolarization to the dynamic capillary occlusions was excluded by continuously monitoring the blood flow with laser speckle contrast imaging, since changes in cerebral perfusion (spreading waves of oligemia) accompany the electrophysiological events driven by the peri-infarct depolarizations.[24–28] Moreover, the capillary stalls were happening without observable fluctuations of flow in large blood vessels, hence being an exclusive phenomenon of the microcirculation (Supplementary Movies 3 and 4).

The main advantage of OCT with this evaluation was its ability to image the flow in several hundred capillaries simultaneously and the very prominent signal change that occurs when capillary RBC flow is halted. Two photon fluorescent angiography in the corresponding areas with frequent and dynamic stalls 2 h after reperfusion showed repetitive plugging of capillaries by cells identified as leukocytes based on their size (Supplementary Movies 5 and 6). We further confirmed these cells were leukocytes but not RBC clusters by staining them with Rhodamine-6G, a mitochondrial stain (Supplementary Movie 7, Supplementary Figure S4). These leukocytes would plug individual capillaries for seconds or minutes, then would squeeze slowly and finally allow flow in that particular capillary again. A single temporary plug could affect the RBC flow in other capillaries in the nearby network, dynamically affecting the propensity of stalls in a greater number of capillaries (Supplementary Movie 6). We hypothesized that capillary flow irregularities introduced by stuck or slowly moving leukocytes would be contributing to the dynamic persistent capillary stalls in the reperfused ischemic penumbra, as if they were slowly moving trucks in a busy traffic. Meanwhile, we did not detect time-dependent increases in capillary stall measurements ($n = 4$) or comparable leukocyte plugging ($n = 2$) in sham animals with nonspecific mechanical compression (that did not target the dMCA) over a 3-h observation period (Supplementary Figure 1, Supplementary Movie 8), making a confounding effect of craniotomy or systemic phenomenon unlikely for our observations on stalls with dMCAO.

Targeting neutrophils by anti-Ly6G monoclonal antibody reduces the stall events in penumbra

We were motivated by a recent study on increased number of capillary flow stalls in a mouse model of Alzheimer's disease[29] that could be resolved by specific targeting of a neutrophil surface protein, Ly6G, using a monoclonal antibody, resulting in improved CBF and cognitive performance within minutes. Ly6G is a glycosylphosphatidylinositol-anchored surface antigen specifically expressed on mouse neutrophils with unknown function.[30,31] With a similar approach, we aimed to improve the dynamic persistent capillary flow interruptions in the penumbra after ischemia–reperfusion by targeting neutrophils with the same type and dose of anti-Ly6G antibodies. Although our primary aim was to identify at least one role player in the increased number of stalls rather than establishing

Figure 2. Continued
Ischemic core is outlined with white dotted line. Scale bars: 500 μm. (g) Sagittal cross-section showing the axial decay of OCT amplitude signal. Solid white structure on the right is the cover glass. There is reduced axial penetration of the OCT signal in the core area. (h) Signal attenuation slope map of the same region imaged simultaneously with (f). Darker pixels indicate higher (more negative) axial signal attenuation slope. Unit of calibration bar is 1/mm^2. (i) The histological infarct shown by lack-of TTC staining of the brain approximately 10 min after the imaging in (i) shows overlap with the zone of reduced signal penetration. (j–l) prD-OCT images of axial velocity in the ischemic penumbra, during baseline, ischemia and reperfusion. Imaging planes are approximately 50 μm below the cortical surface, to get optimal cross-sections of penetrating arterioles. Arterioles and venules could be differentiated by their flow direction, as indicated by different colors. Negative values indicate arterioles and positive values indicate venules. Blood flow values were measured longitudinally in each penetrating arteriole (white circles) for quantification across time points. White arrows show the direction of flow in a distal pial branch of MCA, that was reversed, receiving collateral flow during occlusion and resolved after reperfusion. Scale bars: 100 μm.

Table 1. Physiological parameters.

	Baseline			Ischemia -1h			Reperfusion -1h			Reperfusion -2h		
	Control	Ly6G	Sham	Control	Ly6G	Sham	Control	Ly6G	Sham	Control	Ly6G	Sham
Body temperature (°C)	36.7–37.3 (Homeothermic control)			36.7–37.3 (Homeothermic control)			36.7–37.3 (Homeothermic control)			36.7–37.3 (Homeothermic control)		
Mean arterial pressure (mmHg)	78.9 ± 0.9	76.2 ± 3.7	75.3 ± 1.1	76.1 ± 1.68	75.3 ± 2.3	73.3 ± 1.3	71.8 ± 1.62	67.1 ± 2.9	68.8 ± 3.0	72.7 ± 1.36	70.8 ± 2.8	68.9 ± 3.1
Heart rate (beats per min)	440 ± 15	441 ± 14	427 ± 19	425 ± 16	443 ± 11	428 ± 42	446 ± 17	472 ± 14	426 ± 48	414 ± 24	424 ± 23	443±55
Oxygen saturation (%)	96.9 ± 0.4	97.3 ± 0.4	96.5 ± 0.7	96.6 ± 0.4	97.5 ± 0.4	97.0 ± 0.8	96.9 ± 0.3	97.1 ± 0.6	97.3 ± 0.6	96.0 ± 0.6	97.8 ± 0.2	97.5 ± 0.3

a treatment method with full potential, we also wanted to address the possibility of using anti-Ly6G as an adjunctive target to assist endovascular recanalization. Therefore, we chose to apply the antibody intravenously (2 mg/kg) immediately after recanalization($n = 11$), at the same dose to be effective for improving leukocyte-dependent stalls in the previous study.[29] For controls, the same dose and volume of isotype control antibodies were injected ($n = 13$).

In both Ly6G-targeted and control groups, 1 h after induction of ischemia by dMCA compression, the incidence of stalling capillaries increased almost threefold and the prevalence almost six-fold, indicating that nearly 20% of the visible capillaries (i.e. capillaries exhibiting flowing RBCs at some point during our 6.5 min measurement) were not flowing in the ischemic penumbra at any given time, with a different subset of capillaries flowing at each time point (Figures 3(h) and 4(d) to (f)). This effect of ischemia on stalls was proportionally higher than the 50% reduction in perfused capillaries at any time (Figure 4(c)) (this percentage of capillary perfusion reduction was also in line with previous studies[32]). For the subsequent 2 h after reperfusion, stall incidence, prevalence and cumulative duration, remained statistically higher than baseline in the penumbra (Figures 3(h) and 4(d) to (f)).

Although there was no significant difference between the two treatments in baseline or ischemia (1st h) stalls (therefore the two groups were identical before the antibody administration), we observed a reduction in capillary stalls after reperfusion in the anti-Ly6G group, becoming significant at 2 h and even better differentiated at 24 h after reperfusion (Figures 3(i) and 4(d) to (f)). An improvement in CBF accompanied the improvement in capillary stalls, as measured by prD-OCT (Figure 4(b)). The number of OCT-visible capillaries was not significantly different between the two treatment groups at any time point, but the difference in flow was compensated by a higher capillary velocity and pial arterial velocity in the Ly6G-treated group (Figure 4(g) and (h)). Interestingly, these improvements in CBF and stall dynamics did not depend on a vasodilatory action mediated by anti-Ly6G, as we did not detect any significant difference in relative changes in pial arterial diameters in the penumbral zones (Figure 4(i)). We also did not notice a vascular diameter or blood flow change in a sham animal injected with anti-Ly6G antibody and monitored for up to 3 h after injection (Supplementary Figure S5). The improvements were independent of systemic physiological changes with no significant difference across groups at all-time points (Table 1). We also evaluated the leukocyte and differential neutrophil counts before and after antibody administration. The leukocyte and differential

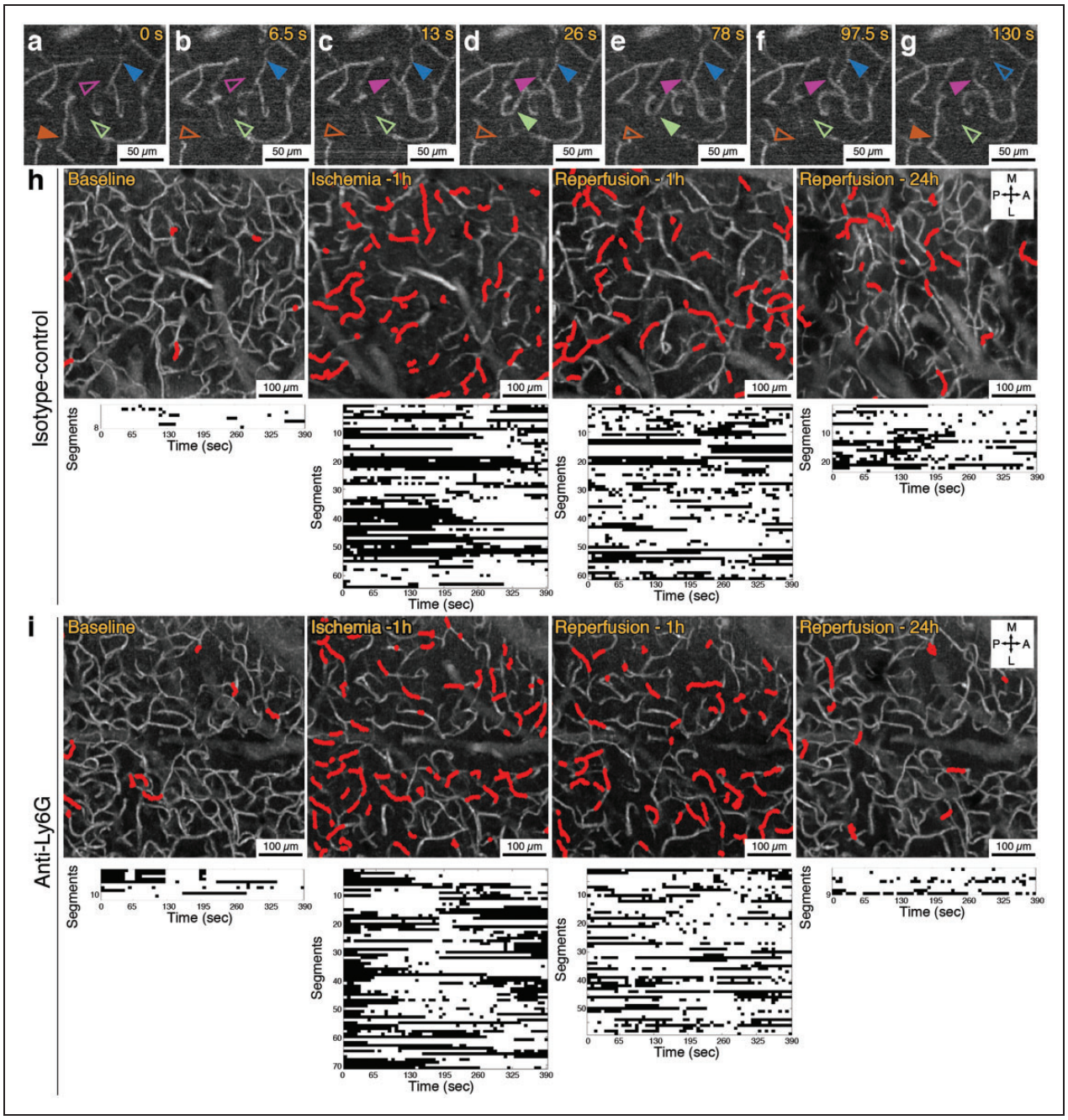

Figure 3. (a–g) Representative OCT angiogram time series showing capillary flow appearing and disappearing repeatedly over an observation period of 130 s in the penumbra, during 1 h of MCA occlusion. Solid arrowheads indicate that the capillary segment is flowing and empty arrowheads indicate that the segment is not flowing at that time point. Scale bars: 50 μm. (h) Capillary angiograms over penumbra zone of an isotype-control injected animal (average of 60 images, acquired over 6.5 min) with the dynamically stalling segments indicated in red. Each stall event measured in these segments is shown in the plots (the bottom row) as black dots. (i) Capillary stall profile in an animal injected with anti-Ly6G antibody immediately after reperfusion. Scale bars in (h) and (i): 100 μm.

neutrophil counts at 2 h after reperfusion and anti-Ly6G treatment was not different from the controls (Figure 4(a)), which is also in line with the previous study on Alzheimer's models with the same monoclonal antibody.[29] At the 24th h however, we saw a prominent reduction in neutrophil count compared to the control antibody-treated group as expected, confirming the specific effect of the anti-Ly6G on neutrophil depletion (Figure 4(a)). The modulatory effect on the stall dynamics at the 1st day therefore could be

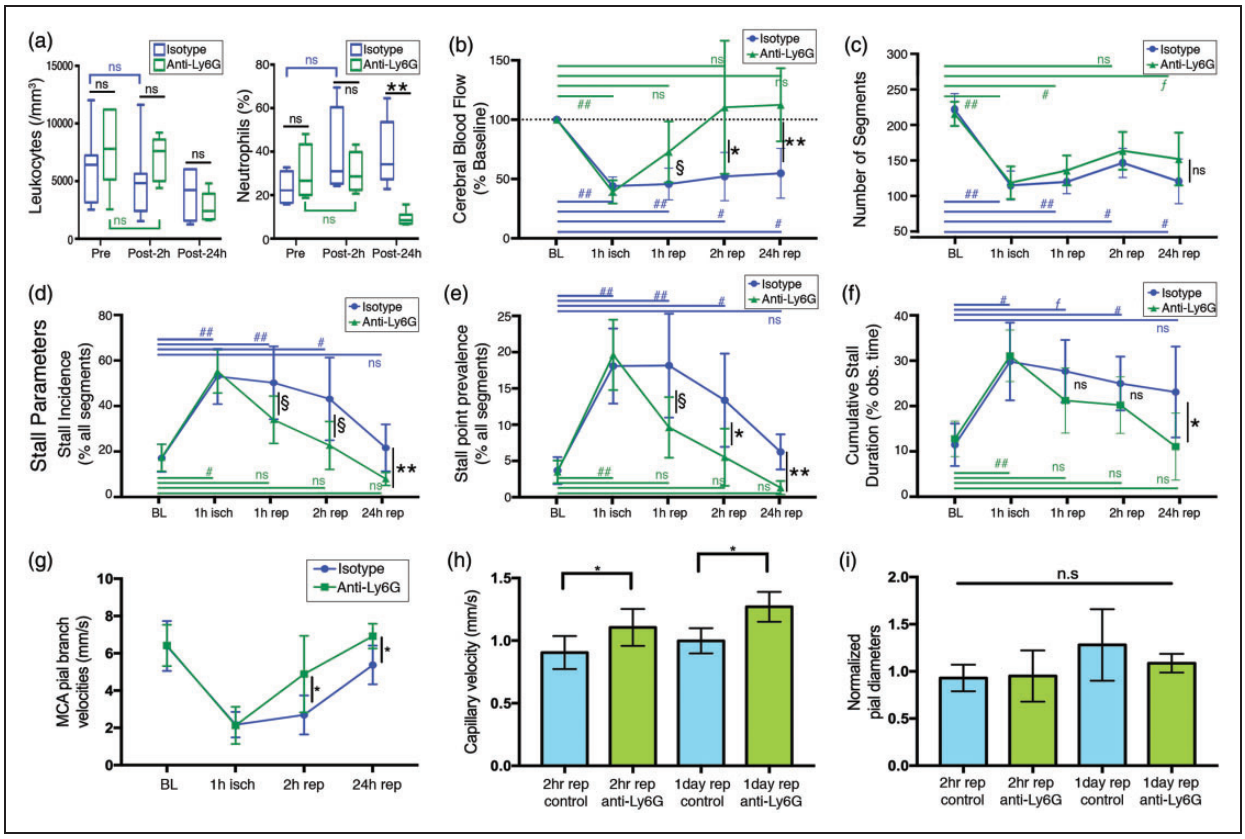

Figure 4. (a) Total leukocyte count was not significantly different in Ly6G group from control at any time point, despite being relatively lower at 24 h. Differential neutrophil count was significantly different between two groups only at the 24-h time point. In control animals, there was a trend of increasing neutrophil counts after ischemia over one day although statistically nonsignificant. Boxes show medians and interquartile range, whiskers show 5–95th percentiles. (b) Penumbral blood flow changes during MCAO and reperfusion in control and Ly6G groups, measured by prD-OCT and expressed as percentage of baseline flow. The decrease in blood flow was almost the same in both treatment groups, but blood flow recovered to a significantly higher level at 2 and 24 h after reperfusion in the Ly6G-treated group (c) Total number of capillary segments in experimental groups in ischemic penumbra, measured at baseline and at different experimental time points. Although the anti-Ly6G group seemed to have a relatively higher number of capillary segments after reperfusion, this difference was not significant. (d–f) Longitudinal monitoring of various stall parameters at different time points during occlusion and reperfusion in ischemic penumbra. Baseline and ischemia conditions were almost identical in control and Ly6G groups, but with an improvement starting (but marginally significant) as early as 1 h, which became significant at 2 h and 24 h after reperfusion. (g–h) MCA pial branch flow velocities and capillary flow velocities were significantly higher in anti-Ly6G-treated animals at 2 h and 24 h after reperfusion. (i) Pial arterial diameters measured from 4th order MCA branches (normalized to baseline diameters) did not show significant changes between treatment groups. Animal counts: For the 24-h timepoint, $n = 6$ for both treatment groups. For the other time points, $n = 13$ and $n = 11$ for control and anti-Ly6G, respectively. Significance: (**) (##) $p < 0.01$, (*)(#) $0.01 \leq p < 0.05$, (*f*)(§) $0.05 \leq p < 0.09$, (n.s.) $p \geq 0.09$.

attributed to a reduction in neutrophil count. However, at the very acute phase as early as 2 h, without any effect in neutrophil counts, we still noticed a significant effect on capillary flow, suggesting that reduction of neutrophil count may not be necessary for the effect to occur.

Improving microcirculation via anti-Ly6G improves functional outcomes and reduces ischemic damage

In addition to quantifying an improvement in microcirculatory parameters after reperfusion with intravenous administration of anti-Ly6G, we further tested if this improvement would be actually beneficial for the ischemic tissue, contributing to the salvaging of penumbra. In a separate group of mice, we first compared the effect of anti-Ly6G antibody ($n = 3$) versus control ($n = 3$) on capillary pO_2 distribution in the acute setting (2 h of reperfusion) with phosphorescence lifetime imaging (Figure 5(a) to (c)). Excessive temporal fluctuations in capillary oxygen pressure in the presence of stalls (between 18 and 65 mmHg over ~2.5 min) (Figure 5(d)) were suggestive for pathological effects of stalls on oxygenation of ischemic microvasculature.

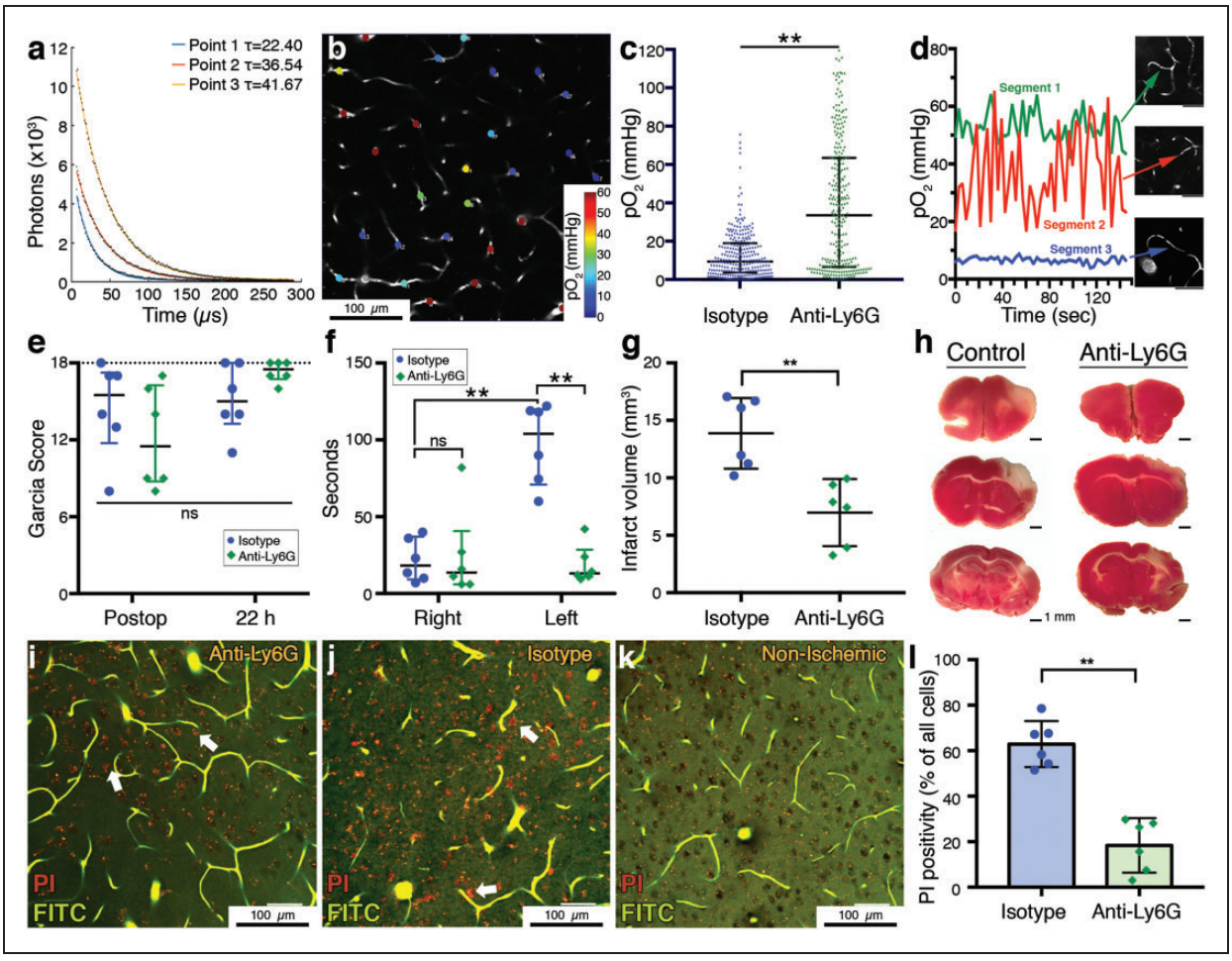

Figure 5. (a) Phosphorescence lifetime measurements at three different points with different decay time constants (τ's) corresponding to different pO_2 values. (b) Two-photon imaging plane showing pO_2 values at measurement points across the microvasculature. Scalebar: 100 μm. (c) Distribution of pO_2 values in measured capillaries in control and Ly6G-treated mice ($n = 3$ per group) showing that anti-Ly6G-treated mice had a significantly higher capillary oxygenation. Data summarized as median-interquartile range. (d) Temporal pO_2 tracings measured at three different capillaries, one with constant flow (segment 1), one with constant stall during the observed time (segment 3) and one with repetitive short-duration stalls (segment 2). pO_2 partial pressure fluctuates prominently in the repeatedly stalling capillary. Scalebars: 50 μm. (e) Garcia neurological scores in the postoperative period, 1 h after recovery from anesthesia was similar in both treatment groups. At 22 h, anti-Ly6G-treated animals had relatively higher scores but the difference was not significant. Maximum possible score of 18 is indicated with the dashed line. Data summarized as median-interquartile range (f) Adhesive tape removal test indicated a significant impairment in control animals compared to the right (unaffected) side, as shown here as the time to tape removal in seconds. This asymmetry disappeared in anti-Ly6G-treated animals. Data shown as median-interquartile range. (g–h) Infarct volumes were significantly lower in anti-Ly6G-treated animals. The cortical area with lack of pink TTC staining demonstrates the irreversibly injured tissue. (i–k) Ex vivo angiograms with red propidium iodide (PI) labeling of injured cells (white arrows) in ischemic periinfarct tissue. These images are maximum intensity projections over 30 μm, at approximately 150 μm depth under cortical surface. Capillaries are visible as they are filled with a fluorescent gel containing FITC (green). Anti-Ly6G-treated animals had less PI labeling compared to controls. No specific PI labeling was observed in nonischemic brain areas (k). Punctate red fluorescence signals originate from lipofuscin granules that are normally found in neurons. Total number of cells was determined by counting of the black circular structures visible in the relatively brighter background on green channel. Scale bars: 50 μm. (l) PI positivity, as expressed by the percentage of all visible cells was significantly lower in anti-Ly6G-treated group. Significance: (**) $p < 0.01$, (*) $0.01 \leq p < 0.05$, (n.s.) $p \geq 0.05$. Sample sizes: $n = 6$ mice for (e–g), $n = 6$ regions over three mice per group in (l), $n = 80$–86 vessels (per animal) for six mice in (c).

We indeed detected a significantly higher oxygen availability in capillaries with anti-Ly6G treatment in ischemic penumbra 2 h after reperfusion (Figure 5(c)).

We then evaluated the functional neurological scores at ~22 h after reperfusion ($n = 6$ per group). Initial Garcia neurological scores of animals that were recorded 1 h after recovery were not significantly different between the two groups and with prominent neurological deficits, suggesting that the initial ischemic insult was comparable between groups (Figure 5(e)).

We saw an improvement indicating functional recovery with the Garcia scores at 22-h for both groups, while the difference was not significantly different between control and anti-Ly6G-treated animals (Figure 5(e)), but we explained this by the relative insensitivity of this scoring system for smaller cortical lesions generated by dMCAO models.[33] To account for fine sensorimotor disturbances, we performed the more sensitive adhesive tape removal test.[34] This test, indeed, revealed a significant delay in tape removal time in the affected limb of the isotype-control animals (Figure 5(f)). In the anti-Ly6G-treated group, the difference between the affected and nonaffected limb was significantly decreased, showing a functional improvement. Moreover, when infarct volumes were determined by 2,3,4-triphenyltetrazolium chloride (TTC) staining in these brains 24 h after ischemia, as a standard procedure for ischemic stroke studies,[35] we saw significantly smaller infarcts in the Ly6G-treated group, consistent with functional scores and microcirculatory parameters (Figure 5(g) and (h)).

Finally, in another group of mice, we wanted to evaluate the cellular damage at periinfarct zones microscopically. The next day after dMCAO and treatment with anti-Ly6G ($n = 3$) or isotype control ($n = 3$), mice were intraperitonally injected with propidium iodide (PI). Four hours later (24 h after reperfusion), they were transcardially perfused with a fluorescent FITC-albumin gel. PI is normally cell impermeable but can pass into the cells if membrane permeability is increased (as in cellular damage), allowing the dye to interact with nucleic acids and become fluorescent. This approach was used previously to stain degenerating neurons in a mouse cerebral ischemia model.[36] Fluorescent gel perfusion and optical index matching allowed high-resolution ex vivo imaging of the microvasculature[37,38] (Figure 5(i) to (k)), while retaining the three dimensional tissue structure. We identified the MCA-supplied region with fluorescent vasculature guidance and detected the injured cells with their PI fluorescence. No specific PI staining was observed in nonischemic zones of the ipsilateral hemisphere (Figure 5(k)). We counted the PI-positive cells at the infarct boundary zone within 500 μm distance to the nonischemic cortex, at 100–200 μm depth (layers II-III) at two different ROIs in each animal. We determined the number of normal nuclei taking advantage of their shadows in the FITC-channel over background (Figure 5(i) to (k)), without distinguishing between neuronal and other cellular nuclei for analysis. We found a significant reduction in the fraction of degenerating cells in this zone of potential for recovery with treatment, in the Ly6G-treated group (Figure 5(l)), as a histological hallmark of the observed effect in microcirculation and functional scores.

Discussion

We present a dynamic mechanism for persistent dysfunctional microcirculation in tissues that can be potentially rescued, along with a possible hyperacute role of intracapillary neutrophil passage in this dysfunction. Technically, systematic evaluation of dynamic capillary stalls was only possible by the high spatiotemporal resolution imaging of OCT angiogram time-series, which clearly indicated flowing RBC signal within hundreds of capillaries simultaneously without labeling. The experimental power of this study arises from the well-controlled and carefully monitored dMCAO and recanalization along with detailed characterization of the ischemic tissue as core and penumbra. The way we distinguish between irreversibly damaged and salvageable tissues was not based simply on CBF changes but on an integrated approach considering capillary perfusion and in vivo optical changes in the tissue with histological validation. The ability to map the signal attenuation across the cortex allowed in vivo demonstration of irreversibly damaged tissue, in line with previous reports on the histologically validated abnormal OCT signal attenuation profile.[20,39] While the exact histopathological hallmark of this optical phenomenon is reserved for future investigation, it was extremely useful for evaluation of the extent of ischemic damage without sacrificing the subject and allowed us to adjust for the natural variability in experimental stroke because of the differences in vascular anatomy and collateral supply. Moreover, unlike other methods of transient dMCAO (like thromboembolic, microclip, suture-ligation, electrocoagulation[40]), we could precisely achieve full recanalization at every attempt with minimal variability. The experimental model can also be considered relevant for an endovascular stroke treatment perspective.

Expanding our previous observations under physiological conditions,[11] we saw that the capillary RBC flow was extremely irregular and intermittent in the ischemic penumbra, with cells repeatedly getting stuck and released in the microcirculation. It is already known that cerebral capillary flow velocities are very different from each other, plasma and RBCs are differentially partitioned at bifurcations,[41] causing a spatial heterogeneity which can lower oxygen extraction efficiency.[10,42–45] Simulations revealed that the flow kinetics and partitioning in the tight lumen of capillaries are dominated by complex physical cell–cell interactions and rheology which are influenced by temporal events affecting the incidental cell distributions.[41] Our findings introduce experimental data on the origins of temporal heterogeneity in individual capillary segments, which can readily influence the interconnected vessels in the network, and cumulatively in a chain-like fashion.[46] As

a slight change in stall dynamics can have a profound impact on the overall microvascular blood flow[47] and oxygenation, this can be considered analogous to a traffic jam formation initiated by slight vehicle movement disturbances in a road network.[13] Our findings suggest that these dynamic disturbances are not simple by-standers of the evolving ischemic core but can contribute to the ongoing tissue damage in potentially recoverable tissues during acute ischemia. This is in line with recent studies showing seizure-related abnormal capillary vasospasms in hippocampus[48] and stagnant capillaries at a distance from occluded penetrating arterioles leading to neurodegeneration.[49] While single rare capillary stalls, as in healthy animals[11] could possibly be tolerated by the capillary network, in high numbers and under oligemic conditions with decreased functional capillary reserve, they can aggravate tissue injury in the initial hours of ischemia. Most importantly, this dysfunction is very profound in the penumbra after reperfusion, which can help explain the extended neurological impairment or less-than-expected clinical benefit.[3] Our data may bring an insight on how selective neuronal necrosis can accumulate in the ischemic penumbra after reperfusion.[50–52] This can cause further functional impairment, by delaying recovery, or lowering cognitive reserve.[51]

Anti-Ly6G antibodies are traditionally used for neutrophil depletion in mice, established within 24 h.[31] We decided to use the neutrophil-targeting approach based on our in vivo TPM observations that leukocytes were dynamically plugging the ischemic capillaries in penumbra, as they were briefly getting stuck and released in microcirculation (Supplementary Movies 3 to 5). We wanted to see if we could improve capillary flow patterns along with tissue survival, in line with recent observations on a mouse model with Alzheimer's disease.[53] It was indeed possible to modulate the capillary stalls with this treatment being applied even after reperfusion, modelling an adjuvant therapy to mechanical thrombectomy. The effect of the antibody was established at 2 h after reperfusion and without the requirement for absolute reduction of neutrophil count.

This is not the first study targeting neutrophils in ischemic stroke and other neurological diseases and the phenomenon of capillary plugs in ischemia by red and white blood cells is not entirely new. Progressively, increasing leukocyte plugging has already been shown in skeletal and myocardial muscle after ischemia and reperfusion, increasing microvascular resistance and negatively affecting the blood flow.[54–56] Neutrophils were previously shown to increase their endothelial adhesion after stroke[19,57] and occlude the capillary bed.[9] Endothelial adhesion molecules like VCAM1 and P-selectin are rapidly upregulated under ischemic conditions for increased leukocyte-endothelium interactions.[19,58,59] Neutrophils can extend tissue injury by permanently occluding capillaries and also by releasing proteases after their recruitment and passage into the brain parenchyma.[7–9,60] Most of the previous studies focused on decreasing the neutrophil counts or limiting recruitment, to prevent tissue damage by their contribution to BBB leakage, reactive oxygen species and toxic enzyme release within the parenchyma.[61] These previous approaches elaborate a possible effect happening over a few days after ischemic induction. Typically, recruitment into brain parenchyma begins 6–8 h after ischemia[61,62] and peaks at 24–48 h.[60,61] The majority of these studies with neutrophil depletion reported a beneficial outcome in animal models.[61] Even the same anti-Ly6G antibody used in this study was found effective for subarachnoid hemorrhage-related vasospasm in one study[63] and improved early parenchymal blood flow in another.[64] Anti-Ly6G also improved functional scores after stroke at 72 h in hyperlipidemic mice.[65] Our results, despite confirming the previously shown effects by neutrophil targeting, should be interpreted differently, as we indicate a rather hyper acute direct effect on dynamic microcirculatory flow patterns with early administration of the anti-Ly6G monoclonal antibody simultaneously with full recanalization. Indeed, in a murine model of neonatal hypoxic-ischemic encephalopathy and lipopolysaccharide challenge, early prophylactic targeting of Ly6G-positive neutrophils prevented neutrophil-associated inflammatory activity and brain damage, while delayed treatment several hours after ischemia was not effective.[66] In line with this recent study that did not evaluate blood flow, our findings indicate a possible contribution of early temporal flow heterogeneity introduced into the microcirculation by neutrophils to the ultimate functional outcome. This suggestion is based on the improvement of capillary flow dynamics as early as 2 h after reperfusion by neutrophil targeting, which is reflected positively to the corresponding capillary oxygenation profile. However, it is not yet possible to attribute the improvement in all outcomes at 24 h, like infarct volume, cellular damage and functional scores solely to the early hemodynamic improvement and clearing of neutrophils from microcirculation, as neutrophil targeting may beneficially affect the final outcome by other mechanisms. These alternative mechanisms may include neutrophil–platelet interactions,[67,68] neutrophil extracellular trap formations,[69,70] activation of coagulation pathways[71] and blood–brain barrier damage and secondary tissue inflammation.[61,72] Thereby, further studies are required to differentially evaluate other components of this microcirculatory dysfunction. Nevertheless, improving the temporary interruptions in capillary flow in the already (but suboptimally)

flowing capillaries may be a compelling target to positively influence the overall cerebral perfusion and oxygen availability, rather than reopening a considerable portion of permanently occluded capillaries to improve the microcirculation.

One limitation of our study was reliance on acute surgical preparations and the necessity to use isoflurane for our long-duration experiments. Although we utilized our best to control for the confounders, monitored systemic physiology, and included proper sham and control groups, we cannot completely exclude any effect of anesthesia or surgical trauma on our observations. Isoflurane, for instance, is a neuroprotectant and has profound effects on CBF.[73–75] The acute craniotomy procedures may have aggravated inflammatory changes in the tissue, increasing leukocyte adhesion.[57] These issues will need to be addressed in future studies, that would be conducted in awake animals with chronic cranial windows. Another limitation was inclusion of relatively young animals to limit the variability related to the factors in the care of animals that can occur throughout lifetime. Since most stroke cases occur in elderly patients with other comorbidities, the extension of this study's findings in such mice with appropriate cardiovascular disease models will be necessary. Although we are well aware of the benefit of both male and female mice for experimental studies, we had to include only male mice here, because the well-documented gender effect on neutrophil function as well as the variability of sex hormones in female mice[76] would increase the number of mice to be used several folds. From our perspective, this was acceptable as we were not proposing a fully established treatment for immediate clinical translation, but we were defining a dynamic pathogenic mechanism in a rather homogeneous sample. It has recently been shown that capillary RBC dynamics show substantial difference between gray and white matter.[77] We were not able address this variation since OCT could not resolve deep white matter capillaries through the cranial window. However, with appropriate optical approaches, the stall phenomenon can be studied in white matter ischemia-reperfusion in comparison with cortex. Finally, and maybe the most importantly, our therapeutic target, the Ly6G protein, is expressed in mice and not in humans.[78] Therefore, this molecular target is not directly applicable for human use. Since Ly6G's endogenous ligand and physiological role are still unknown, it will take time before we identify a working candidate for human use. Deciphering the mechanism of this antibody was beyond the scope of this research but proposes an interesting question for investigators in the field. At least for now, the strong association of neutrophil/lymphocyte ratio in blood with clinical severity in stroke patients is encouraging for our observations.[79,80]

It can be argued that the effect on capillary flow was generated by induced leukopenia, with less cells in circulation that can potentially occlude the capillaries. Anti-Ly6G antibodies provide specific identification of neutrophils and also induce neutropenia in mice 24 h after their administration.[31,81] However, we noticed a significant effect as early as 2 h after reperfusion, even before the settlement of neutropenia. This implies that absolute reduction of neutrophil counts may not be necessary for the effect. We are cautious about making interpretations about any effect of anti-Ly6G on neutrophil adhesion, size or flexibility, before they are fully depleted, as we did not make a systematic investigation for these. Nevertheless, Ly6G targeting was previously suggested to decrease the endothelial adhesion of neutrophils by the downregulation of β2-integrins on the surface.[82]

These findings, in our opinion, help better understanding the dynamic capillary flow issues in cerebral ischemia. It may be useful to take these brief but frequent and persistent 'traffic jams' into consideration while interpreting any structural change in microcirculation or any change in hematological parameters. This improvement in the field may lead to novel strategies to improve overall cellular passage through the microcirculation to enhance the clinical benefits of endovascular treatment. Possible targets may not be just limited to neutrophils and can also include deformability of blood cells, endothelial surface protein expression and reactive oxygen species. We believe that recognition of this dynamic phenomenon can catalyze more basic and clinical research broadly for acute neurological disorders in the near future.

Funding

The author(s) disclosed receipt of the following financial support for the research, authorship, and/or publication of this article: This study was supported by National Institute of Health grants R01-EB021018 and R01-NS108472. Şefik Evren Erdener's work was supported by Turkish Neurological Society and Hacettepe University Scientific Research Projects Coordination Unit (TUI-2019-18106). Dmitry Postnov was supported by Novo Nordisk Foundation, Denmark (NNF17OC0025224).

Authors' note

Şefik E Erdener is now affiliated with Hacettepe University, Institute of Neurological Sciences and Psychiatry, Ankara, Turkey.

Acknowledgements

We would like to thank Andrew Dunn for laser speckle acquisition software, Sergei Vinogradov for providing phosphorescent probes and Michael Moskowitz for helpful discussion. We also thank Blaire Lee for the technical assistance.

Declaration of conflicting interests

The author(s) declared no potential conflicts of interest with respect to the research, authorship, and/or publication of this article.

Authors' contributions

SEE conceived the study objectives, designed and performed the experiments, acquired, processed and analyzed the data, wrote the manuscript. JT set up and optimized the OCT equipment, wrote acquisition codes and processing algorithms. KK designed the surgical procedures and performed experiments. DP set up and optimized the laser speckle imaging equipment, SK wrote data analysis codes, analyzed data. AC and JG set up and optimized two-photon microscope, prepared data analysis codes and performed the experiments. TV performed experiments, acquired and analyzed data. SS and CBS contributed to study objectives and experimental design and critically evaluated the manuscript. DAB supervised the project in overall, contributed to study objectives and experimental design, and critically evaluated the manuscript.

Data availability

The data sets generated during and/or analyzed during the current study, raw image files, custom MATLAB codes used to process and analyze data and their detailed usage instructions are available from the corresponding author upon request. MATLAB scripts can also be found at https://github.com/BUNPC.

ORCID iD

Şefik E Erdener https://orcid.org/0000-0002-5141-7899

Supplemental material

Supplemental material for this article is available online.

References

1. Powers WJ, Rabinstein AA, Ackerson T, et al. 2018 guidelines for the early management of patients with acute ischemic stroke: a guideline for healthcare professionals from the American Heart Association/American Stroke Association. *Stroke* 2018; 49: e46–e99.
2. Shang X, Lin M, Zhang S, et al. Clinical outcomes of endovascular treatment within 24 hours in patients with mild ischemic stroke and perfusion imaging selection. *Am J Neuroradiol* 2018; 39: 1083–1087.
3. El Amki M and Wegener S. Improving cerebral blood flow after arterial recanalization: a novel therapeutic strategy in stroke. *Int J Mol Sci* 2017; 18: pii: E2669.
4. Soares BP, Chien JD and Wintermark M. MR and CT monitoring of recanalization, reperfusion, and penumbra salvage: everything that recanalizes does not necessarily reperfuse! *Stroke* 2009; 40: S24–S27.
5. Dalkara T and Arsava EM. Can restoring incomplete microcirculatory reperfusion improve stroke outcome after thrombolysis. *J Cereb Blood Flow Metab* 2012; 32: 2091–2099.
6. Yemisci M, Gursoy-Ozdemir Y, Vural A, et al. Pericyte contraction induced by oxidative-nitrative stress impairs capillary reflow despite successful opening of an occluded cerebral artery. *Nat Med* 2009; 15: 1031–1037.
7. Perez-de-Puig I, Miró-Mur F, Ferrer-Ferrer M, et al. Neutrophil recruitment to the brain in mouse and human ischemic stroke. *Acta Neuropathol* 2015; 129: 239–257.
8. Neumann J, Riek-Burchardt M, Herz J, et al. Very-late-antigen-4 (VLA-4)-mediated brain invasion by neutrophils leads to interactions with microglia, increased ischemic injury and impaired behavior in experimental stroke. *Acta Neuropathol* 2015; 129: 259–277.
9. del Zoppo GJ, Schmid-Schönbein GW, Mori E, et al. Polymorphonuclear leukocytes occlude capillaries following middle cerebral artery occlusion and reperfusion in baboons. *Stroke* 1991; 22: 1276–83.
10. Østergaard L, Jespersen SN, Mouridsen K, et al. The role of the cerebral capillaries in acute ischemic stroke: the extended penumbra model. *J Cereb Blood Flow Metab* 2013; 33: 635–648.
11. Erdener ŞE, Tang J, Sajjadi A, et al. Spatio-temporal dynamics of cerebral capillary segments with stalling red blood cells. *J Cereb Blood Flow Metab* 2019; 39: 886–900.
12. Hogg JC. Neutrophil kinetics and lung injury. *Physiol Rev* 1987; 67: 1249–95.
13. Jiang R, Hu M-B, Zhang HM, et al. Traffic experiment reveals the nature of car-following. *PLoS One* 2014; 9: e94351.
14. Arsava EM, Gurer G, Gursoy-Ozdemir Y, et al. A new model of transient focal cerebral ischemia for inducing selective neuronal necrosis. *Brain Res Bull* 2009; 78: 226–231.
15. Srinivasan VJ, Jiang JY, Yaseen MA, et al. Rapid volumetric angiography of cortical microvasculature with optical coherence tomography. *Opt Lett* 2010; 35: 43.
16. Tang J, Erdener SE, Fu B, et al. Capillary red blood cell velocimetry by phase-resolved optical coherence tomography. *Opt Lett* 2017; 42: 3976–3979.
17. Sakadžić S, Roussakis E, Yaseen MA, et al. Cerebral blood oxygenation measurement based on oxygen-dependent quenching of phosphorescence. *J Vis Exp* 2011; 51: 1694.
18. Taskiran-Sag A, Yemisci M, Gursoy-Ozdemir Y, et al. Improving microcirculatory reperfusion reduces parenchymal oxygen radical formation and provides neuroprotection. *Stroke* 2018; 49: 1267–1275.
19. Quenault A, Martinez de Lizarrondo S, Etard O, et al. Molecular magnetic resonance imaging discloses endothelial activation after transient ischaemic attack. *Brain* 2017; 140: 146–157.

20. Srinivasan VJ, Mandeville ET, Can A, et al. Multiparametric, longitudinal optical coherence tomography imaging reveals acute injury and chronic recovery in experimental ischemic stroke. *PLoS One* 2013; 8: e71478.
21. Prosser J, Butcher K, Allport L, et al. Clinical-diffusion mismatch predicts the putative penumbra with high specificity. *Stroke* 2005; 36: 1700–1704.
22. Copen WA, Schaefer PW and Wu O. MR perfusion imaging in acute ischemic stroke. *Neuroimaging Clin N Am* 2011; 21: 259–83, x.
23. Ayata C, Dunn AK, Gursoy-OZdemir Y, et al. Laser speckle flowmetry for the study of cerebrovascular physiology in normal and ischemic mouse cortex. *J Cereb Blood Flow Metab* 2004; 24: 744–55.
24. Shin HK, Dunn AK, Jones PB, et al. Vasoconstrictive neurovascular coupling during focal ischemic depolarizations. *J Cereb Blood Flow Metab* 2006; 26: 1018–30.
25. Strong AJ, Anderson PJ, Watts HR, et al. Peri-infarct depolarizations lead to loss of perfusion in ischaemic gyrencephalic cerebral cortex. *Brain* 2007; 130: 995–1008.
26. Lückl J, Dreier JP, Szabados T, et al. Peri-infarct flow transients predict outcome in rat focal brain ischemia. *Neuroscience* 2012; 226: 197–207.
27. Bere Z, Obrenovitch TP, Bari F, et al. Ischemia-induced depolarizations and associated hemodynamic responses in incomplete global forebrain ischemia in rats. *Neuroscience* 2014; 260: 217–26.
28. Dreier JP, Fabricius M, Ayata C, et al. Recording, analysis, and interpretation of spreading depolarizations in neurointensive care: review and recommendations of the COSBID research group. *J Cereb Blood Flow Metab* 2017; 37: 1595–1625.
29. Cruz Hernández JC, Bracko O, Kersbergen CJ, et al. Neutrophil adhesion in brain capillaries reduces cortical blood flow and impairs memory function in Alzheimer's disease mouse models. *Nat Neurosci* 2019; 22: 413–420.
30. Fleming TJ, Fleming ML and Malek TR. Selective expression of Ly-6G on myeloid lineage cells in mouse bone marrow. RB6-8C5 mAb to granulocyte-differentiation antigen (Gr-1) detects members of the Ly-6 family. *J Immunol* 1993; 151: 2399–408.
31. Daley JM, Thomay AA, Connolly MD, et al. Use of Ly6G-specific monoclonal antibody to deplete neutrophils in mice. *J Leukoc Biol* 2008; 83: 64–70.
32. Ennis SR, Keep RF, Schielke GP, et al. Decrease in perfusion of cerebral capillaries during incomplete ischemia and reperfusion. *J Cereb Blood Flow Metab* 1990; 10: 213–220.
33. Schaar KL, Brenneman MM, Savitz SI, et al. Functional assessments in the rodent stroke model. *Exp Transl Stroke Med* 2010; 2: 13.
34. Bouet V, Boulouard M, Toutain J, et al. The adhesive removal test: a sensitive method to assess sensorimotor deficits in mice. *Nat Protoc* 2009; 4: 1560–1564.
35. Liu F, Schafer DP and McCullough LD. TTC, fluoro-Jade B and NeuN staining confirm evolving phases of infarction induced by middle cerebral artery occlusion. *J Neurosci Methods* 2009; 179: 1–8.
36. Cevik U and Dalkara T. Intravenously administered propidium iodide labels necrotic cells in the intact mouse brain after injury [1]. *Cell Death Differ* 2003; 10: 928–929.
37. Ke M-T, Fujimoto S and Imai T. SeeDB: a simple and morphology-preserving optical clearing agent for neuronal circuit reconstruction. *Nat Neurosci* 2013; 16: 1154–1161.
38. Tsai PS, Kaufhold JP, Blinder P, et al. Correlations of neuronal and microvascular densities in murine cortex revealed by direct counting and colocalization of nuclei and vessels. *J Neurosci* 2009; 29: 14553–14570.
39. Baran U, Li Y and Wang RK. In vivo tissue injury mapping using optical coherence tomography based methods. *Appl Opt* 2015; 54: 6448.
40. McCabe C, Arroja MM, Reid E, et al. Animal models of ischaemic stroke and characterisation of the ischaemic penumbra. *Neuropharmacology* 2018; 134(Pt B): 167–177.
41. Balogh P and Bagchi P. Analysis of red blood cell partitioning at bifurcations in simulated microvascular networks. *Phys Fluids* 2018; 30: 051902.
42. Moeini M, Lu X, Avti PK, et al. Compromised microvascular oxygen delivery increases brain tissue vulnerability with age. *Sci Rep* 2018; 8: 1–17.
43. Østergaard L, Aamand R, Karabegovic S, et al. The role of the microcirculation in delayed cerebral ischemia and chronic degenerative changes after subarachnoid hemorrhage. *J Cereb Blood Flow Metab* 2013; 33: 1825–1837.
44. Jespersen SN and Østergaard L. The roles of cerebral blood flow, capillary transit time heterogeneity, and oxygen tension in brain oxygenation and metabolism. *J Cereb Blood Flow Metab* 2012; 32: 264–277.
45. Engedal TS, Hjort N, Hougaard KD, et al. Transit time homogenization in ischemic stroke – a novel biomarker of penumbral microvascular failure? *J Cereb Blood Flow Metab* 2018; 38: 2006–2020.
46. Fu X, Gens JS, Glazier JA, et al. Progression of diabetic capillary occlusion: a model. *PLoS Comput Biol* 2016; 12: 1–46.
47. Nishimura N, Schaffer CB, Friedman B, et al. Targeted insult to subsurface cortical blood vessels using ultrashort laser pulses: three models of stroke. *Nat Methods* 2006; 3: 99–108.
48. Leal-Campanario R, Alarcon-Martinez L, Rieiro H, et al. Abnormal capillary vasodynamics contribute to ictal neurodegeneration in epilepsy. *Sci Rep* 2017; 7: 1–14.
49. Taylor ZJ, Hui ES, Watson AN, et al. Microvascular basis for growth of small infarcts following occlusion of single penetrating arterioles in mouse cortex. *J Cereb Blood Flow Metab* 2016; 36: 1357–73.
50. Guadagno JV, Jones PS, Aigbirhio FI, et al. Selective neuronal loss in rescued penumbra relates to initial hypoperfusion. *Brain* 2008; 131: 2666–2678.
51. Baron J-C, Yamauchi H, Fujioka M, et al. Selective neuronal loss in ischemic stroke and cerebrovascular disease. *J Cereb Blood Flow Metab* 2014; 34: 2–18.
52. Phan TG, Wright PM, Markus R, et al. Salvaging the ischaemic penumbra: more than just reperfusion? *Clin Exp Pharmacol Physiol* 2002; 29: 1–10.

53. Cruz Hernández JC, Bracko O, Kersbergen CJ, et al. Neutrophil adhesion in brain capillaries reduces cortical blood flow and impairs memory function in Alzheimer's disease mouse models. *Nat Neurosci* 2019; 22: 413–420.
54. Harris AG and Skalak TC. Effects of leukocyte activation on capillary hemodynamics in skeletal muscle. *Am J Physiol* 1993; 264: H909–916.
55. Harris AG and Skalak TC. Effects of leukocyte capillary plugging in skeletal muscle ischemia-reperfusion injury. *Am J Physiol* 1996; 271: H2653–2660.
56. Helmke BP, Bremner SN, Zweifach BW, et al. Mechanisms for increased blood flow resistance due to leukocytes. *Am J Physiol Circ Physiol* 2017; 273: H2884–H2890.
57. Clark WM, Coull BM, Briley DP, et al. Circulating intercellular adhesion molecule-1 levels and neutrophil adhesion in stroke. *J Neuroimmunol* 1993; 44: 123–125.
58. Fournier AP, Quenault A, Martinez de Lizarrondo S, et al. Prediction of disease activity in models of multiple sclerosis by molecular magnetic resonance imaging of P-selectin. *Proc Natl Acad Sci U S A* 2017; 114: 6116–6121.
59. Gauberti M, Montagne A, Marcos-Contreras OA, et al. Ultra-sensitive molecular MRI of vascular cell adhesion molecule-1 reveals a dynamic inflammatory penumbra after strokes. *Stroke* 2013; 44: 1988–1996.
60. Garcia JH, Liu KF, Yoshida Y, et al. Influx of leukocytes and platelets in an evolving brain infarct (Wistar rat). *Am J Pathol* 1994; 144: 188–199.
61. Jickling GC, Liu D, Ander BP, et al. Targeting neutrophils in ischemic stroke: translational insights from experimental studies. *J Cereb Blood Flow Metab* 2015; 35: 888–901.
62. Watcharotayangul J, Mao L, Xu H, et al. Post-ischemic vascular adhesion protein-1 inhibition provides neuroprotection in a rat temporary middle cerebral artery occlusion model. *J Neurochem* 2012; 123: 116–124.
63. Provencio JJ, Altay T, Smithason S, et al. Depletion of Ly6G/C(+) cells ameliorates delayed cerebral vasospasm in subarachnoid hemorrhage. *J Neuroimmunol* 2011; 232: 94–100.
64. Neulen A, Pantel T, Kosterhon M, et al. Neutrophils mediate early cerebral cortical hypoperfusion in a murine model of subarachnoid haemorrhage. *Sci Rep* 2019; 9: 1–10.
65. Herz J, Sabellek P, Lane TE, et al. Role of neutrophils in exacerbation of brain injury after focal cerebral ischemia in hyperlipidemic mice. *Stroke* 2015; 46: 2916–2925.
66. Yao H-W and Kuan C-Y. Early neutrophil infiltration is critical for inflammation-sensitized hypoxic-ischemic brain injury in newborns. *J Cereb Blood Flow Metab* , Epub ahead of print 16 December 2019. DOI: 10.1177/0271678X19891839.
67. Denorme F, Manne BK, Portier I, et al. Platelet necrosis mediates ischemic stroke outcome in mice. *Blood* 2019; 135: 429–440.
68. García-Culebras A, Durán-Laforet V, Peña-Martínez C, et al. Myeloid cells as therapeutic targets in neuroinflammation after stroke: specific roles of neutrophils and neutrophil-platelet interactions. *J Cereb Blood Flow Metab* 2018; 38: 2150–2164.
69. Kim S-W, Lee H, Lee H-K, et al. Neutrophil extracellular trap induced by HMGB1 exacerbates damages in the ischemic brain. *Acta Neuropathol Commun* 2019; 7: 94.
70. Manda-Handzlik A and Demkow U. The brain entangled: the contribution of neutrophil extracellular traps to the diseases of the central nervous system. *Cells* 2019; 8: pii: E1477.
71. Massberg S, Grahl L, von Bruehl M-L, et al. Reciprocal coupling of coagulation and innate immunity via neutrophil serine proteases. *Nat Med* 2010; 16: 887–896.
72. Jian Z, Liu R, Zhu X, et al. The involvement and therapy target of immune cells after ischemic stroke. *Front Immunol* 2019; 10: 2167.
73. Li L and Zuo Z. Isoflurane preconditioning improves short-term and long-term neurological outcome after focal brain ischemia in adult rats. *Neuroscience* 2009; 164: 497–506.
74. Matta BF, Heath KJ, Tipping K, et al. Direct cerebral vasodilatory effects of sevoflurane and isoflurane. *Anesthesiology* 1999; 91: 677–680.
75. Sun M, Deng B, Zhao X, et al. Isoflurane preconditioning provides neuroprotection against stroke by regulating the expression of the TLR4 signalling pathway to alleviate microglial activation. *Sci Rep* 2015; 5: 11445.
76. Ahnstedt H, McCullough LD and Cipolla MJ. The importance of considering sex differences in translational stroke research. *Transl Stroke Res* 2016; 7: 261–273.
77. Li B, Ohtomo R, Thunemann M, et al. Two-photon microscopic imaging of capillary red blood cell flux in mouse brain reveals vulnerability of cerebral white matter to hypoperfusion. *J Cereb Blood Flow Metab* 2020; 40: 501–512.
78. Lee PY, Wang J-X, Parisini E, et al. Ly6 family proteins in neutrophil biology. *J Leukoc Biol* 2013; 94: 585–594.
79. Maestrini I, Strbian D, Gautier S, et al. Higher neutrophil counts before thrombolysis for cerebral ischemia predict worse outcomes. *Neurology* 2015; 85: 1408–1416.
80. Fang Y-N, Tong M-S, Sung P-H, et al. Higher neutrophil counts and neutrophil-to-lymphocyte ratio predict prognostic outcomes in patients after non-atrial fibrillation-caused ischemic stroke. *Biomed J* 2017; 40: 154–162.
81. Bruhn KW, Dekitani K, Nielsen TB, et al. Ly6G-mediated depletion of neutrophils is dependent on macrophages. *Results Immunol* 2016; 6: 5–7.
82. Wang J-X, Bair AM, King SL, et al. Ly6G ligation blocks recruitment of neutrophils via a β2-integrin-dependent mechanism. *Blood* 2012; 120: 1489–1498.